Hybrid NOMA/OMA Broadcasting-and-Buffer-State-Based Relay Selection

Jun Kochi, Ryota Nakai, *Student Member, IEEE*, and Shinya Sugiura, *Senior Member, IEEE*

***Abstract*—In this paper, we propose a novel buffer-aided relay selection scheme that is capable of amalgamating the concepts of non-orthogonal multiple access (NOMA) and orthogonal multiple access (OMA) in the context of two-hop cooperative networks supporting multiple relays. This is enabled by allowing relay nodes to share a common information packet in their buffers with the aid of a source-to-relay broadcasting mode. Hence, the proposed relay selection scheme switches between diverse modes of uplink NOMA, downlink NOMA, unicast, source broadcasting, and cooperative beamforming. The theoretical bounds of the outage probability, throughput, average delay, and diversity order are derived for the proposed scheme, based on a Markov chain model. Through our analytical and numerical results, it is demonstrated that the proposed scheme is capable of switching to one of the best modes in an adaptive manner while outperforming the conventional buffer-aided cooperative schemes.**

***Index Terms*—Adaptive transmission, broadcast, buffer, cooperative network, delay, markov chain, NOMA, outage probability, relay selection, theoretical analysis.**

I. Introduction

NON-ORTHOGONAL multiple access (NOMA) [1]–[5] enables flexible resource allocation in comparison to the conventional orthogonal multiple access (OMA) counterpart. The benefits of NOMA are achieved at the cost of increased detection complexity imposed on the receivers. More specifically, multiuser superposition coding and successive interference cancellation (SIC), used in a NOMA scenario, allow us to exploit a diverse combination of independent channels in an adaptive manner. This implies that the achievable performance gain of NOMA over OMA depends on the channel condition. Hence, in order to efficiently achieve the benefits of NOMA, in [6]–[8], adaptive NOMA/OMA mode switching was developed for massive MIMO systems. While the original NOMA was proposed for the multiuser downlink scenario [1], it was applicable to both the downlink and uplink scenarios [9]; the two modes are referred to as downlink (DL)-NOMA and uplink (UL)-NOMA [10], respectively.

Relay-aided cooperative communications have been extensively investigated [11]–[14]. In a two-hop relay network where multiple relay nodes are positioned sufficiently apart from each other, source-to-relay (SR) and relay-to-destination (RD) channels are typically uncorrelated, and hence the spatial diversity order, corresponding to the number of relay nodes, is achievable. Furthermore, for the sake of improving the achievable diversity gain of cooperative communications, the exploitation of data buffers at relay nodes was considered for two-hop cooperative networks [15]–[19], whose achievable diversity order increases to up to twice that of the conventional ones that do not rely on data buffers. Note that the performance gain of the buffer-aided cooperative schemes was achievable at the cost of increased end-to-end communication delay as well as additional overhead imposed by pilot transmission and channel monitoring. In [20], Nomikos *et al.* developed the reduced-complexity buffer-aided link selection algorithm with outdated channel state information (CSI) and feedback errors.

In [21]–[24], the buffer-aided relay selection was combined with NOMA. More specifically, in [21], Luo and Teh considered adaptive downlink transmission with a single buffer-aided relay node while employing NOMA in the relaying phase. In [22], adaptive use of UL-NOMA and OMA was proposed in the context of buffer-aided relaying uplink, where two users communicate with a single relay node with hybrid NOMA/OMA transmission, while the buffer-aided relay nodes retransmit the received packet to a destination node. Furthermore, in [23], Alkhawatrah *et al.* propose a novel prioritization-based buffer-aided relay selection scheme that combines the NOMA and OMA modes in the Internet of Things (IoT) downlink, where NOMA is exploited in the relaying phase.

Moreover, in [25]–[30], broadcasting an information packet from a source node to multiple relay nodes was introduced in the context of the aforementioned buffer-aided cooperative communications; this allows relay nodes to share a common information packet, hence increasing the degree of freedom in buffer states. As a result, the source-to-destination (SD)

Manuscript received October 28, 2020; revised December 15, 2020 and January 18, 2021; accepted January 24, 2021. Date of publication January 27, 2021; date of current version March 10, 2021. This work was supported in part by the Japan Society for the Promotion of Science (JSPS) KAKENHI under Grants 16KK0120, 17H03259, and 17K18871 and in part by JST PRESTO under Grant JPMJPR1933. The review of this article was coordinated by Prof. Y. Gao. *(Corresponding author: Shinya Sugiura.)*

Jun Kochi is with the Department of Computer and Information Sciences, Tokyo University of Agriculture and Technology, Koganei 184-8588, Japan (e-mail: jnkch810@gmail.com).

Ryota Nakai is with the Institute of Industrial Science, The University of Tokyo, Tokyo 153-8505, Japan (e-mail: rnakai@g.ecc.u-tokyo.ac.jp).

Shinya Sugiura is with the Institute of Industrial Science, The University of Tokyo, Tokyo 153-8505, Japan, and also with the Japan Science and Technology Agency (JST), Kawaguchi 332-0012, Japan (e-mail: sugiura@ieee.org).

Digital Object Identifier 10.1109/TVT.2021.3054904

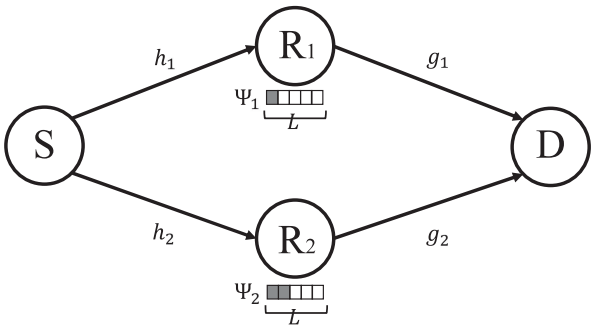

Fig. 1. System model of the proposed two-hop buffer-aided cooperative scheme.

communication delay was kept at the minimum while achieving the high reliability of buffer-aided relay selection. Such broadcasting- and buffer-state-based (BBSB) relay selection schemes were developed in the context of decode-and-forward (DF) [25] and amplify-and-forward (AF) relaying scenarios [26]. Furthermore, the cooperative beamforming mode was incorporated into BBSB relay selection in [27], while BBSB relay selection was introduced to physical-layer security [28], NOMA [29], and cognitive radio networks [30]. Note that, the conventional BBSB schemes of [25]–[28] does not rely on NOMA. Also, while in [29], the DL-NOMA concept was incorporated into the relaying phase of the buffer-aided relay selection for the multi-user downlink, cooperative beamforing and the NOMA mode in the source transmission phase were not exploited.

In the context of the above, the novel contributions of the present paper are as follows.

- We propose a novel multi-mode BBSB relay selection scheme which amalgamates two NOMA modes (DL-NOMA and UL-NOMA) and three OMA modes (broadcast, unicast, and cooperative beamforming), allowing hybrid exploitation of NOMA and OMA in a seamless manner. While the main benefits of the proposed scheme are achieved by the NOMA concept, which allows us to send simultaneously send superimposed symbols, hence enhancing the transmission rate. However, in order to successfully decode the superimposed signals at the receiver(s), the associated SNR has to be sufficiently high. Hence, the NOMA and OMA modes are switched, depending on the link conditions.
- Our DL-NOMA mode in the SR transmission phase superimposes multiple different packets for the transmission to the relay nodes, while the broadcast mode allows the relay nodes to share a packet. Additionally, our cooperative beamforming mode in the RD relaying phase becomes realistic by relying on a packet share in the buffers of the relay nodes.
- Furthermore, in order to validate the system model of the proposed scheme, we derive the theoretical throughput, outage probability, delay, and diversity order based on the Markov chain model. Through our analytical and numerical performance results, it is demonstrated that the proposed scheme is capable of successfully switching to one of the best modes in an adaptive manner, hence outperforming the conventional buffer-aided cooperative schemes.

The remainder of this paper is organized as follows. We present the system model of the proposed hybrid NOMA/OMA BBSB relay selection scheme in Section II, and the associated link selection algorithm is proposed in Section III. In Section IV, we derive the theoretical bounds of throughput, outage probability, delay, and diversity order. In Section V, we provide our performance results, and in Section VI, we conclude the present paper.

II. System Model

Let us consider a two-hop relaying network consisting of a single source node S, two relay nodes R_1 and R_2, and a single destination node D, as shown in Fig. 1. However, the proposed scheme is readily applicable to the scenario of an arbitrary number of relay nodes. We assume that there is no direct link between the source and the destination nodes, where each node is equipped with a single antenna element. The channel coefficients of the first and the second SR links are denoted as h_1 and h_2, while those of the first and the second RD links are represented by g_1 and g_2. Also, each relay node operates in the half-duplex mode under the DF principle, while having a data buffer of finite size L. The numbers of packets stored in the buffers of the first and the second relay nodes are represented by Ψ_1 and Ψ_2. Furthermore, all the SR and RD links are modeled as independent and identically distributed (IID) Rayleigh fading, where the channel coefficients are random variables following the Gaussian distribution with a zero mean and unit variance.

Similar to [1]–[3], we also assume that the CSI of all the links and the buffer state information (BSI) of the relay nodes are collected at a central coordinator. Based on the collected CSI and BSI, the central coordinator determines which link or link subset is activated. The modes in the proposed scheme are classified into NOMA and OMA modes, which are employed both for the SR transmission and the RD relaying phases. More specifically, as shown in Fig. 2, the proposed scheme contains six modes: two OMA-based SR transmission modes, a single NOMA-based SR transmission mode, two OMA-based RD relaying modes, and a single NOMA-based RD relaying mode. In each mode, the transmission rate per packet is fixed at r_0 [bps/Hz]. In an RD relaying phase, if the destination node successfully decodes the received packet, an acknowledge (ACK) packet is sent back to both the relay nodes with low-rate feedback links, and the associated packet is deleted from the buffers of the relay nodes.

A. DL-NOMA Mode for SR Transmission Phase

Fig. 2(a) shows the DL-NOMA mode for the SR transmission phase. In this mode, the source node simultaneously multicasts packets to both the relay nodes, by multiplexing two source packets into a single packet, according to the DL-NOMA principle [1]–[3]. More specifically, the superimposed information signal x is represented by

$$x = \sqrt{a_1}x_1 + \sqrt{a_2}x_2, \tag{1}$$

where x_i $(i \in \{1, 2\})$ represent packets transmitted to the relay nodes with the average power of $\mathbb{E}[|x_i|^2] = 1$. It is assumed that

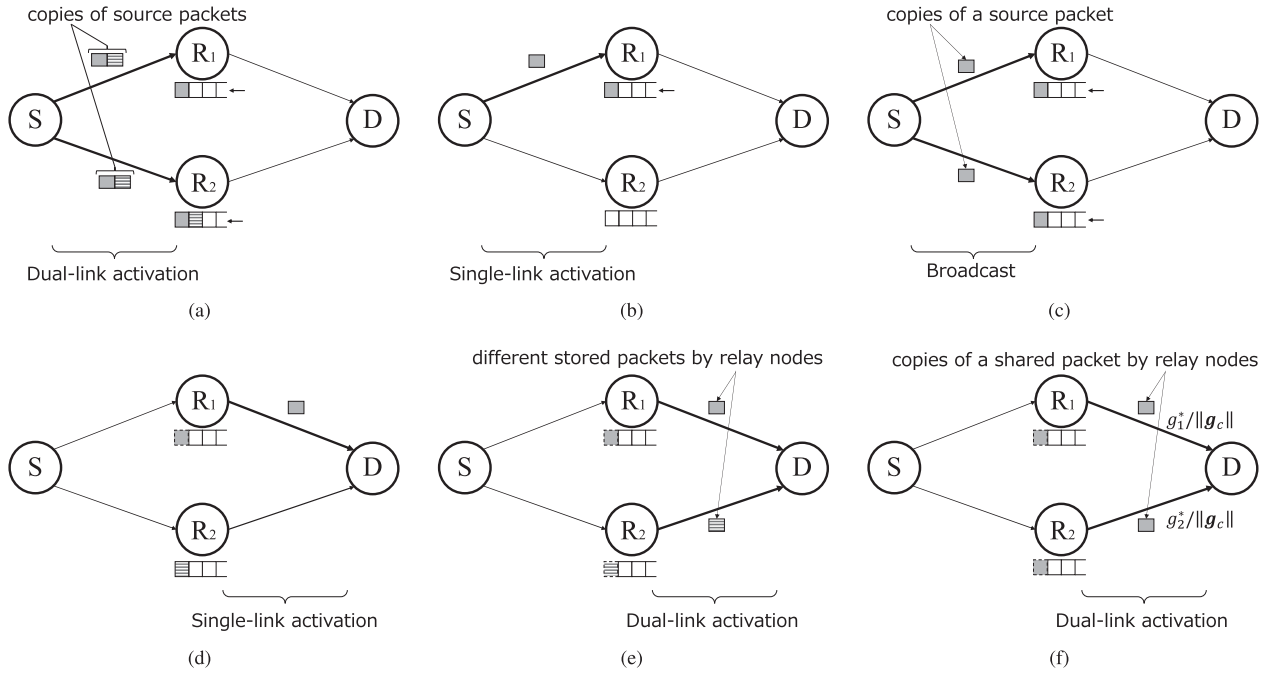

Fig. 2. Six transmission modes, composed of four OMA modes and two NOMA modes. (a) DL-NOMA mode for SR transmission phase. (b) Unicast mode for SR transmission phase. (c) Broadcast mode for SR transmission phase. (d) Unicast mode for RD relaying phase. (e) UL-NOMA mode for RD relaying phase. (f) Cooperative beamforming mode for RD relaying phase

the symbol rates of x_1 and x_2 are the same. Furthermore, a_i $(0 \leq a_i \leq 1)$ denotes the power allocation coefficient corresponding to x_i, where we have the total power constraint of

$$\sum a_i \leq 1. \tag{2}$$

Since in this mode two packets are simultaneously transmitted, the sum transmission rate is given by $2r_0$. Then, the signal received at the kth relay node is given by

$$y_k^{\mathrm{SR}} = h_k \sqrt{P_s} x + n_k, \tag{3}$$

where P_s denotes the transmit power of the source node, and n_k denotes the associated additive white Gaussian noise (AWGN) component, which has variance δ_R^2.

Here, we assume that the first and the second SR links are the sub and the main links, which are determined as introduced later in Section III-B. In this case, the first relay node decodes a single packet x_1, while the second relay node decodes two packets x_1 and x_2. More specifically, the second relay node decodes the multiplexed packets in descending order, i.e., first x_1 and then x_2, with the aid of SIC.

The capacity between the source node and the kth relay node in terms of the source symbol x_1 is expressed as

$$\mathcal{C}_{\mathrm{DL}_1}^{\mathrm{SR}}(h_k) = \frac{1}{2} \log_2 \left(1 + \frac{|h_k|^2 a_1 \gamma_{\mathrm{SR}}}{|h_k|^2 a_2 \gamma_{\mathrm{SR}} + 1} \right), \tag{4}$$

where the transmit power corresponding to x_2, i.e., $a_2 P_s$, is regarded as an interference power. Also, γ_{SR} denotes the average SNR of the two SR links, which is calculated by $\gamma_{\mathrm{SR}} = P_s / {\delta_R}^2$. Since each relay node operates in the half-duplex mode, a pre-log factor of 1/2 is imposed on the capacity expression.

Then, if we have

$$\mathcal{C}_{\mathrm{DL}_1}^{\mathrm{SR}}(h_1) \geq r_0, \tag{5}$$

the first relay node successfully decodes x_1. Similarly, if we have

$$\mathcal{C}_{\mathrm{DL}_1}^{\mathrm{SR}}(h_2) \geq r_0, \tag{6}$$

the second relay node decodes x_1. Furthermore, in order for the second relay node to decode x_2 in addition to x_1, the received signal is modified based on the SIC principle as follows:

$$\begin{aligned} \bar{y}_2^{\mathrm{SR}} &= y_2^{\mathrm{SR}} - h_2 \sqrt{P_s a_1} x_1 \\ &= h_2 \sqrt{P_s a_2} x_2 + n_2. \end{aligned} \tag{7}$$

Under the assumption that x_1 is successfully decoded and SIC is used at the second relay node, the associated capacity in terms of x_2 is given by

$$\mathcal{C}_{\mathrm{DL}_2}^{\mathrm{SR}}(h_2) = \frac{1}{2} \log_2 \left(1 + |h_2|^2 a_2 \gamma_{\mathrm{SR}} \right). \tag{8}$$

Finally, if we have

$$\mathcal{C}_{\mathrm{DL}_2}^{\mathrm{SR}}(h_2) \geq r_0, \tag{9}$$

the second relay node can decode x_2. Note that in order to successfully decode x_2 at the second relay node with the aid of SIC, x_1 has to be decoded in advance. Hence, both the conditions (6) and (9) have to be satisfied. In order to avoid the outage event in this DL-NOMA scenario, all the inequalities (5), (6), and (9) have to be satisfied.

The central coordinator calculates the optimal power allocation coefficients a_1 and a_2 based on the collected CSI. From (4),

(5), and (6), we arrive at

$$a_1 \geq \frac{\gamma_t(|h_k|^2 a_2\gamma_{\rm SR}+1)}{|h_k|^2\gamma_{\rm SR}} \quad (k=1,2), \tag{10}$$

while, from (8) and (9), we obtain

$$a_2 \geq \frac{\gamma_t}{|h_2|^2\gamma_{SR}}, \tag{11}$$

where we have $\gamma_t = 2^{2r_0}-1$.

If $|h_1|^2 \leq |h_2|^2$, the two inequalities of (10) for $k=1,2$ are represented by

$$a_1 \geq \frac{\gamma_t(|h_1|^2 a_2\gamma_{\rm SR}+1)}{|h_1|^2\gamma_{\rm SR}} \tag{12}$$

$$= \frac{\gamma_t(a_2\gamma_{\rm SR}+\frac{1}{|h_1|^2})}{\gamma_{\rm SR}} \tag{13}$$

$$\geq \frac{\gamma_t(|h_2|^2 a_2\gamma_{\rm SR}+1)}{|h_2|^2\gamma_{\rm SR}}. \tag{14}$$

Hence, we have the power allocation factors of

$$a_1 = \frac{\gamma_t(|h_1|^2 a_2\gamma_{\rm SR}+1)}{|h_1|^2\gamma_{\rm SR}} \tag{15}$$

$$a_2 = \frac{\gamma_t}{|h_2|^2\gamma_{\rm SR}}. \tag{16}$$

Similarly, if $|h_2|^2 \leq |h_1|^2$, the power allocation factors are given by

$$a_1 = \frac{\gamma_t(|h_2|^2 a_2\gamma_{\rm SR}+1)}{|h_2|^2\gamma_{\rm SR}} \tag{17}$$

$$a_2 = \frac{\gamma_t}{|h_2|^2\gamma_{SR}}. \tag{18}$$

If a_1 and a_2 satisfy the power constraint $a_1+a_2 \leq 1$, the DL-NOMA mode is successful. Otherwise, i.e., if $a_1+a_2>1$, the DL-NOMA mode becomes outage.

B. Unicast Mode for SR Transmission Phase

Fig. 2(b) shows the unicast mode for the SR transmission phase, where either of the two SR links is activated. Hence, in this mode, a single source packet is stored only at the buffer of the activated relay node. The capacity of the kth relay node is represented by

$$\mathcal{C}_{\rm Uni}^{\rm SR}(h_k) = \frac{1}{2}\log_2\left(1+|h_k|^2\gamma_{\rm SR}\right). \tag{19}$$

If $\mathcal{C}_{\rm Uni}^{\rm SR}(h_k) \geq r_0$ and the buffer of the kth relay node is not full, then the unicast mode of the kth SR link can be activated.

C. Broadcast Mode for SR Transmission Phase

Fig. 2(c) shows the broadcasting mode for the SR transmission phase, where the source node simultaneously broadcasts a single source packet to both the relay nodes. Then, when both the relay nodes successfully decode the packet, it is stored at the buffer of each relay node. If the capacities of both the SR links are higher than the transmission rate r_0, i.e.,

$$\mathcal{C}_{\rm Uni}^{\rm SR}(h_1) \geq r_0, \mathcal{C}_{\rm Uni}^{\rm SR}(h_2) \geq r_0, \tag{20}$$

then this broadcast mode can be activated, assuming that the buffers of both the relay nodes have sufficient available slots, as described in Section III-C.

Note that our DL-NOMA and broadcast modes allow the two relay nodes to share a common packet in their buffers. Such a buffer state cannot be achievable in the previous buffer-aided relay selection scheme that does not use the broadcast mode, and this buffer state enables the cooperative beamforming mode of Section II-F. Furthermore, the broadcast mode contributes to the decrease of delay in comparison to the unicast mode [25].

D. Unicast Mode for RD Relaying Phase

Fig. 2(d) shows the unicast mode for the RD relaying phase, where either of the two relay nodes is selected for relaying a packet stored in its buffer. The capacity of the kth RD link is given by

$$\mathcal{C}_{\rm Uni}^{\rm RD}(g_k) = \frac{1}{2}\log_2\left(1+|g_k|^2\gamma_{\rm RD}\right), \tag{21}$$

where $\gamma_{\rm RD}$ denotes the average SNR of the RD links, calculated by $\gamma_{\rm RD} = P_r/\delta_D^2$ with the transmit power of P_r at the activated relay node and the noise variance δ_D^2 at the destination node. This mode can be activated when $\mathcal{C}_{\rm Uni}^{\rm RD}(g_k) > r_0$ and the buffer of the kth relay node is not employed.

E. UL-NOMA Mode for RD Relaying Phase

Fig. 2(e) shows the UL-NOMA mode for the RD relaying phase, where both of the two relay nodes simultaneously transmit different packets to the destination node, packets z_1 and z_2, respectively.

Without loss of generality, let us assume $|g_1|^2 \geq |g_2|^2$. Then, the received signal at the destination node is represented by

$$y^{\rm RD} = g_1\sqrt{P_r b_1}z_1 + g_2\sqrt{P_r b_2}z_2 + n_D, \tag{22}$$

where b_1 and b_2 are the power coefficients of the first and the second relay nodes, respectively, and $(b_1+b_2)P_r$ is the total transmit power of the two relay nodes.[1] More specifically, the maximum total power transmitted from relay nodes is given by P_r, hence having the constraint of $b_1+b_2 \leq 1$.[2] Also, n_D is the corresponding noise component. In order to first decode the packet z_1, the packet z_2 is assumed to be a noise in SIC at the destination node. The associated information rate with respect

[1] In our UL-NOMA mode, power allocation, rather than equal-power relaying of $b_1 = b_2$, is carried out for each relay node, similar to UL-NOMA of [10], [31], [32].

[2] The conventional UL-NOMA of [22], [33] assumed that the maximum transmit power P_r for each user, i.e., the constraint of $b_1 \leq 1$ and $b_2 \leq 1$, which is different from $b_1+b_2 \leq 1$ employed in this paper. In the proposed scheme, a single-user cooperative scenario with multiple relay nodes is considered. The UL-NOMA mode of the proposed scheme is one of the three RD relaying modes, i.e., the unicast, the UL-NOMA, and the cooperative beamforming modes. Hence, to maintain the same total transmit power in each of the three RD relaying modes, the constraint of $b_1+b_2 \leq 1$ is employed.

to x_1 is expressed as

$$\mathcal{C}_{\mathrm{UL}_1}^{\mathrm{RD}}(g_1,g_2)=\frac{1}{2}\log_2\left(1+\frac{|g_1|^2 b_1\gamma_{\mathrm{RD}}}{|g_2|^2 b_2\gamma_{\mathrm{RD}}+1}\right). \tag{23}$$

Then, the information rate of x_2 after successfully decoding x_1 is given by

$$\mathcal{C}_{\mathrm{UL}_2}^{\mathrm{RD}}(g_2)=\frac{1}{2}\log_2\left(1+|g_2|^2 b_2\gamma_{\mathrm{RD}}\right). \tag{24}$$

Similar to the DL-NOMA mode in the SR transmission phase, we have the doubled sum transmission rate of $2r_0$ in this mode.

Moreover, the central coordinator calculates the power allocation coefficients b_1 and b_2 based on the collected CSI. This mode can be activated when $\mathcal{C}_{\mathrm{UL}_1}^{\mathrm{RD}}(g_1,g_2)\geq r_0$ and $\mathcal{C}_{\mathrm{UL}_2}^{\mathrm{RD}}(g_2)\geq r_0$, i.e.,

$$b_1\geq\frac{\gamma_t(|g_2|^2 b_2\gamma_{\mathrm{RD}}+1)}{|g_1|^2\gamma_{\mathrm{RD}}}, \tag{25}$$

$$b_2\geq\frac{\gamma_t}{|g_2|^2\gamma_{RD}}. \tag{26}$$

Hence, the UL-NOMA mode is successful only if the power allocation factors of

$$b_1=\frac{\gamma_t(\gamma_t+1)}{|g_1|^2\gamma_{\mathrm{RD}}} \tag{27}$$

$$b_2=\frac{\gamma_t}{|g_2|^2\gamma_{RD}} \tag{28}$$

satisfy the power constraint of $b_1+b_2\leq 1$. Otherwise, the UL-NOMA mode becomes outage.

The power allocation coefficients b_1 an b_2 may be calculated at a central coordinator, and conveyed to the first and the second relay nodes, respectively.

F. Cooperative Beamforming Mode for RD Relaying Phase

Fig. 2(f) shows the cooperative beamforming mode for the RD relaying phase, where a common packet is simultaneously transmitted from both the relay nodes. As presented in the SR transmission phase, the DL-NOMA mode and the SR broadcasting mode simultaneously activates both the SR links and allows the two relay nodes to share a packet, hence enabling the cooperative beamforming mode.

The transmission weight of the ith relay node is given by $w_i=g_i^*/\|\boldsymbol{g}_c\|$, where we have $\boldsymbol{g}_c=[g_1,g_2]^T$. The associated information rate is given by

$$\mathcal{C}_{\mathrm{Col}}^{\mathrm{RD}}(g_1,g_2)=\frac{1}{2}\log_2\left(1+\|\boldsymbol{g}_c\|^2\gamma_{\mathrm{RD}}\right). \tag{29}$$

Naturally, in the RD relaying phase, the cooperative beamforming mode has a higher performance than the unicast mode, without imposing any performance penalty. However, this mode can be activated when $\mathcal{C}_{\mathrm{Col}}^{\mathrm{RD}}(g_1,g_2)>r_0$ and a specific packet is shared among the two relay nodes.

TABLE I
PRIORITY CLASSIFICATION

Priority	Low	Medium	High
SR link	$\Psi_k=L-1$	$\xi_{\mathrm{SR}}<\Psi_k<L-1$	$\Psi_k\leq\xi_{\mathrm{SR}}$
RD link	$\Psi_k=1$	$1<\Psi_k<\xi_{\mathrm{RD}}$	$\xi_{\mathrm{RD}}\leq\Psi_k$

III. Proposed Link Selection Algorithm

In this section, we present our proposed relay selection algorithm. First, we show the selection algorithm of a single main link. Then, we present our mode selection algorithm.

A. Priority Classification of Each Link

The central coordinator evaluates the priorities of all the SR links and the RD links based on Table I; the priorities are classified into three categories. Two thresholds, ξ_{SR} and ξ_{RD}, are introduced to avoid detrimental buffer states, such as the full and empty buffer states. The ranges of these thresholds are given by $1\leq\xi_{\mathrm{SR}}<\xi_{\mathrm{RD}}\leq L-1$. For example, the priority of the kth SR link is categorized as low if $\Psi_k=L-1$, medium if $\xi_{\mathrm{SR}}<\Psi_k<L-1$, and high if $\Psi_k\leq\xi_{\mathrm{SR}}$. Similarly, the priority of the kth RD link is categorized as low if $\Psi_k=1$, medium if $1<\Psi_k<\xi_{\mathrm{RD}}$, and high if $\xi_{\mathrm{RD}}\leq\Psi_k$. Note that, when the buffer state of kth relay node is full (i.e., $\Psi_k=L$) or empty (i.e., $\Psi_k=0$), the associate SR or RD link cannot be activated, respectively. Therefore, these links are excluded from the candidates to be selected.

Note that the thresholds ξ_{SR} and ξ_{RD} allow us to strike a tradeoff between the throughput, the outage probability, and the average packet delay. If ξ_{SR} and ξ_{RD} are set small, the number of packets stored in the buffer is kept low. This may be beneficial in terms of keeping the average packet delay low since the time packets are held in the buffer is reduced. However, the expected number of available RD links decreases due to the low number of packets stored in the buffers, which may increase the outage probability. By contrast, if the thresholds ξ_{SR} and ξ_{RD} are set high, the number of available RD links increases. As a result, the outage probability decreases, at the cost of the increased average packet delay.

B. Main Link Selection

Based on the priorities of the links, a single link out of four is selected as the main link in each time slot. The priority of the main link selection is in the order of the high-priority SR links, the high-priority RD links, the medium-priority SR links, the medium-priority RD links, the low-priority RD links, and the low-priority SR links. If there are multiple available links in the same priority category, the single strongest link among them is selected.

When the central coordinator verifies that the unicast transmission of the selected main link is in outage, the next available link is selected according to the above-mentioned selection priority.

Having determined the main link, a sub link is set to another link in the same transmission phase. For example, when the

second RD link is selected as a main link, the first RD link is set to a sub link.

C. Mode Selection for SR Transmission Phase

In this section, we consider mode selection for the case where the main link is an SR link, which corresponds to the SR transmission phase. Table II shows the mode selection criterion, where one of the DL-NOMA, broadcast, and unicast modes is activated. Here, let us define the relay node associated with the main link as the main relay node and the other relay node as the sub relay node. Moreover, the numbers of packets stored in the buffers of the main and the sub relay nodes are represented by $\Psi_{\rm main}$ and $\Psi_{\rm sub}$, respectively.

More specifically, when $\Psi_{\rm sub} \geq L-1$, the unicast mode is selected, where a single packet is transmitted to the main relay node (Case 1). This is for the sake of avoiding the detrimental full buffer state at the sub relay node. When $\Psi_{\rm main} = L-1$ and $\Psi_{\rm sub} \leq L-2$, the broadcast mode is activated (Case 2); in this case, the source node simultaneously broadcasts one packet to both the relay nodes. When $\Psi_{\rm main} \leq L-2$ and $\Psi_{\rm sub} \leq L-1$, the DL-NOMA mode is activated (Case 3). If the DL-NOMA mode is outage, the source node broadcasts one packet to both the relay nodes (Case 4). When the main-relay node can receive no packets in Cases 1, 2, and 4, the SR transmission phase experiences an outage event.

D. Mode Selection for RD Relaying Phase

In this section, we consider mode selection for the scenario where the main link is an RD link, which corresponds to the RD relaying phase. Note that $\Psi_{\rm main} \geq 1$ is guaranteed in this scenario. Table III lists the mode selection criterion, which includes six cases.

Let us consider $\Psi_{\rm sub} \geq 2$ and that the two relay nodes share one or more packets. Then, the UL-NOMA mode is activated (Case 1), unless it becomes outage. Otherwise, the cooperative beamforming mode is activated (Case 2). When we have $\Psi_{\rm sub} \geq 1$ and there are no shared packets among the relay nodes, the UL-NOMA mode is activated (Case 3). If Case 3 corresponds to an outage event, the unicast mode is activated (Case 4). If $\Psi_{\rm sub} = 1$ and there is a single shared packet among the relay nodes, the cooperative beamforming mode is activated (Case 5). Finally, when $\Psi_{\rm sub} = 0$. the unicast mode is activated (Case 6).

E. Example of Our Mode Selection

In order to elaborate further, let us exemplify the proposed scheme by using the specific scenario shown in Fig. 3, where the buffer size of each relay node is $L = 4$, the buffer states are $\Psi_1 = 2$ and $\Psi_2 = 1$, and there are no shared packets among the two relay nodes. Furthermore, the threshold parameters are $\xi_{\rm SR} = 1$ and $\xi_{\rm RD} = 2$.

First, the priorities of the four links, i.e., the first SR link, the second SR link, the first RD link, and the second RD link, are determined to be medium, high, high, and low, according to Table I. Next, based on the main link criterion of Section III-B, the second SR link is selected as the main link. Then, according to Table II, the DL-NOMA mode (Case 3) or the broadcast mode may be activated, depending on the channel conditions. More specifically, if the channel conditions of the two SR links are sufficiently high, such that the DL-NOMA mode is not outage, the DL-NOMA mode is activated, as shown in Section II-A. Otherwise, the broadcast mode is activated.

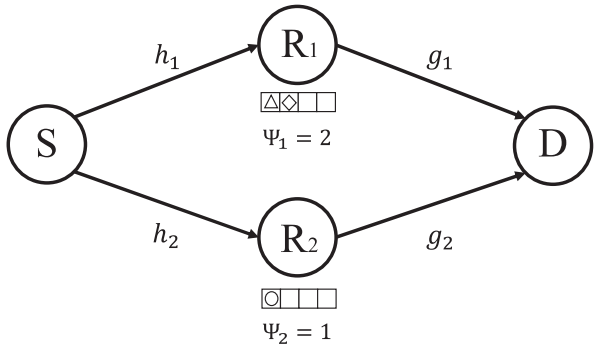

Fig. 3. Example of $L = 4$ where the first relay has two packets and the second relay has one packet. There are no shared packets among the relay nodes.

TABLE II
MODE SELECTION IN SR TRANSMISSION PHASE

	Buffer states	DL-NOMA	Broadcast	Unicast
Case 1	$\Psi_{\rm sub} \geq L-1$	—	—	active
Case 2	$\Psi_{\rm main} = L-1$ $\Psi_{\rm sub} \leq L-2$	—	active	—
Case 3	$\Psi_{\rm main} \leq L-2$	active	—	—
Case 4	$\Psi_{\rm sub} \leq L-2$	fail	active	—

TABLE III
MODE SELECTION IN RD RELAYING PHASE

	Buffer states	UL-NOMA	Cooperative beamforming	Unicast
Case 1	$\Psi_{\rm sub} \geq 2$ & at least one shared packet	active	—	—
Case 2		fail	active	—
Case 3	$\Psi_{\rm sub} \geq 1$ & no shared packet	active	—	—
Case 4		fail	—	active
Case 5	$\Psi_{\rm sub} = 1$ & one shared packet	—	active	—
Case 6	$\Psi_{\rm sub} = 0$	—	—	active

F. Overhead for Monitoring CSI and BSI

Let us evaluate the overhead required for the central coordinator to monitor the CSI and BSI, which are used to select an appropriate link. For simplicity, we assume that the destination node acts as a central coordinator, similar to [25].

In the proposed scheme, all of the SR and RD channels, as well as the BSI of the relay nodes, are updated in each time slot. The source node broadcasts a pilot block to the relay nodes, and each relay node carries out CSI estimation based on the received pilot block. Then, the CSI of the kth SR channel is transmitted to the destination node together with the BSI of the kth relay node. Also, each relay node transmits a pilot block to the destination node, and the destination node then estimates the CSI of the

RD links. Note that the proposed scheme's overhead is the same as those of the conventional generalized max-link and max-link schemes, which are listed in Table II of [25].

The CSI overhead may be reduced when the channel coherence time is longer than the packet interval. Further reduction of overhead remains an open problem for all the buffer-aided relay selection family, including the proposed scheme.

IV. Derivation of Theoretical Bounds

In this section, we derive the theoretical bounds of the throughput, the outage probability, the average packet delay, and the diversity order for the proposed scheme. Our theoretical analysis is based on a Markov chain model, similar to conventional studies [25], [27], [29]. For example, for the scenario of two relay nodes with a buffer size of $L = 2$, we have 19 states, as shown in Table III of [25]. For the sake of simplicity, only the cooperative beamforming is kept deactivated in our analysis. More specifically, we replace the cooperative beamforming mode by the unicast mode.[3] First, we calculate the transition probability of each mode, and then, the state transition matrix of a Markov chain model is defined in order to derive the theoretical bounds.

A. Channel Condition for Successful Transmission

1) DL-NOMA Mode for SR Transmission Phase: In the DL-NOMA mode, the transmission is successful if the power allocation factors of (15), (16) or those of (17), (18) satisfy the power constraint of (2).

If $|h_{\rm main}|^2 \geq |h_{\rm sub}|^2$, from (15) and (16), then (2) can be rewritten as

$$\frac{\gamma_t(|h_{\rm sub}|^2 a_2 \gamma_{\rm SR} + 1)}{|h_{\rm sub}|^2 \gamma_{\rm SR}} + \frac{\gamma_t}{|h_{\rm main}|^2 \gamma_{\rm SR}} \leq 1 \tag{30}$$

$$\Leftrightarrow \frac{|h_{\rm main}|^2 \gamma_t}{|h_{\rm main}|^2 \gamma_{\rm SR} - \gamma_t(\gamma_t+1)} \leq |h_{\rm sub}|^2 \leq |h_{\rm main}|^2. \tag{31}$$

Furthermore, (31) can be modified to

$$\frac{\gamma_t(\gamma_t+2)}{\gamma_{\rm SR}} \leq |h_{\rm main}|^2. \tag{32}$$

Therefore, in order to achieve successful transmission in the DL-NOMA mode, both (31) and (32) have to be satisfied for $|h_{\rm main}|^2$ and $|h_{\rm sub}|^2$. We assume that the channel coefficients are random variables, following the zero-mean unit-variance Gaussian distribution, and hence the probability $P_{\mathcal{D}^1_{\rm DL}}$, satisfying the channel condition for the successful transmission of the DL-NOMA mode, is expressed as

$$\begin{aligned} P_{\mathcal{D}^1_{\rm DL}} &= \int_{\frac{\gamma_t(\gamma_t+2)}{\gamma_{\rm SR}}}^{\infty} \int_{\frac{x\gamma_t}{x\gamma_{\rm SR}-\gamma_t(\gamma_t+1)}}^{x} e^{-x}e^{-y}{\rm d}y{\rm d}x \\ &= \int_{\frac{\gamma_t(\gamma_t+2)}{\gamma_{\rm SR}}}^{\infty} \exp\left(-\frac{x^2\gamma_{\rm SR} - x{\gamma_t}^2}{x\gamma_{\rm SR} - \gamma_t(\gamma_t+1)}\right){\rm d}x \end{aligned}$$

[3]Note that the proposed scheme, including the cooperative beamforming mode, is expressed in the Markov chain model, similar to that without cooperative beamforming. Therefore, the analytical framework derived in this section is readily applicable to the proposed scheme with the cooperative beamforming mode.

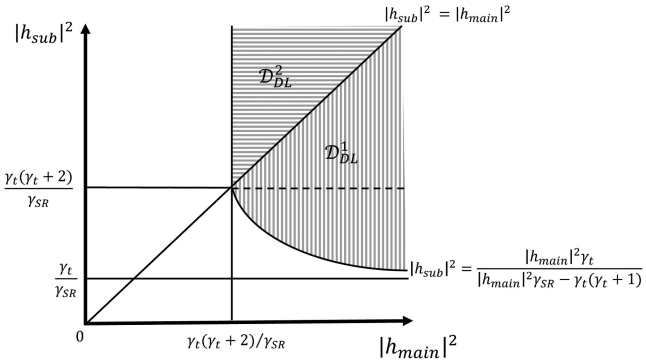

Fig. 4. Region $\mathcal{D}^1_{\rm DL}$ corresponding to the successful transmissions in our DL-NOMA mode under the assumption of $|h_{\rm main}|^2 \geq |h_{\rm sub}|^2$ and region $\mathcal{D}^2_{\rm DL}$ with $|h_{\rm main}|^2 \leq |h_{\rm sub}|^2$.

$$= \frac{1}{2}\exp\left(-\frac{2\gamma_t(\gamma_t+2)}{\gamma_{\rm SR}}\right). \tag{33}$$

Similarly, if $|h_{\rm main}|^2 \leq |h_{\rm sub}|^2$, from (2), (17), and (18), we arrive at the condition of successful transmission of the DL-NOMA mode as follows:

$$\frac{\gamma_t(|h_{\rm main}|^2 a_2 \gamma_{\rm SR} + 1)}{|h_{\rm main}|^2 \gamma_{\rm SR}} + \frac{\gamma_t}{|h_{\rm main}|^2 \gamma_{\rm SR}} \leq 1 \tag{34}$$

$$\Leftrightarrow \frac{\gamma_t(\gamma_t+2)}{\gamma_{\rm SR}} \leq |h_{\rm main}|^2 \tag{35}$$

$$\leq |h_{\rm sub}|^2. \tag{36}$$

Then, the probability $P_{\mathcal{D}^2_{\rm DL}}$, which is associated with the channel condition imposed by the successful transmission of the DL-NOMA mode, is formulated as

$$\begin{aligned} P_{\mathcal{D}^2_{\rm DL}} &= \int_{\frac{\gamma_t(\gamma_t+2)}{\gamma_{\rm SR}}}^{\infty} \int_{\frac{\gamma_t(\gamma_t+2)}{\gamma_{\rm SR}}}^{x} e^{-x}e^{-y}{\rm d}y{\rm d}x \\ &= \frac{1}{2}\exp\left(-\frac{2\gamma_t(\gamma_t+2)}{\gamma_{\rm SR}}\right). \end{aligned} \tag{37}$$

Fig. 4 shows the areas $\mathcal{D}^1_{\rm DL}$ and $\mathcal{D}^2_{\rm DL}$, which correspond to the successful transmissions in our DL-NOMA mode under the assumption of $|h_{\rm main}|^2 \geq |h_{\rm sub}|^2$ and $|h_{\rm main}|^2 \leq |h_{\rm sub}|^2$, respectively.

2) UL-NOMA Mode for RD Relaying Phase: The probability of the channel condition imposed by the successful transmission in the UL-NOMA mode is calculated similarly to the preceding case of the DL-NOMA mode. If $|g_{\rm main}|^2 \geq |g_{\rm sub}|^2$, from (27) and (28), the total power constraint $b_1 + b_2 \leq 1$ is represented by

$$\frac{\gamma_t(\gamma_t+1)}{|g_{\rm main}|^2 \gamma_{\rm RD}} + \frac{\gamma_t}{|g_{\rm sub}|^2 \gamma_{\rm RD}} \leq 1$$

$$\Leftrightarrow \frac{|g_{\rm main}|^2 \gamma_t}{|g_{\rm main}|^2 \gamma_{\rm RD} - \gamma_t(\gamma_t+1)} \leq |g_{\rm sub}|^2 \leq |g_{\rm main}|^2. \tag{38}$$

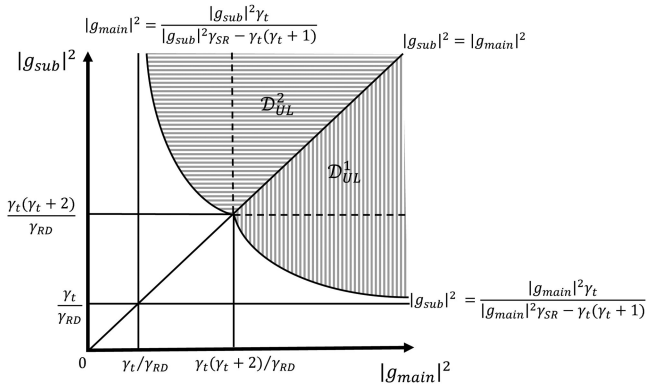

Fig. 5. Region $\mathcal{D}_{\rm UL}^1$ corresponding to the successful transmissions in our DL-NOMA mode under the assumption of $|g_{\rm main}|^2 \geq |g_{\rm sub}|^2$ and region $\mathcal{D}_{\rm UL}^2$ with $|g_{\rm main}|^2 \leq |g_{\rm sub}|^2$.

Moreover, (38) is modified in terms of $g_{\rm main}$ as follows:

$$\frac{\gamma_t(\gamma_t+2)}{\gamma_{\rm RD}} \leq |g_{\rm main}|^2. \tag{39}$$

Thus, the probability $P_{\mathcal{D}_{\rm UL}^1}$ satisfying the channel condition needed for successful transmission in the UL-NOMA mode is given by

$$\begin{aligned} P_{\mathcal{D}_{\rm UL}^1} &= \int_{\frac{\gamma_t(\gamma_t+2)}{\gamma_{\rm RD}}}^{\infty} \int_{\frac{x\gamma_t}{x\gamma_{\rm RD}-\gamma_t(\gamma_t+1)}}^{x} e^{-x}e^{-y}{\rm d}y{\rm d}x \\ &= \int_{\frac{\gamma_t(\gamma_t+2)}{\gamma_{\rm RD}}}^{\infty} \exp\left(-\frac{x^2\gamma_{\rm RD} - x{\gamma_t}^2}{x\gamma_{\rm RD}-\gamma_t(\gamma_t+1)}\right){\rm d}x \\ &\quad - \frac{1}{2}\exp\left(-\frac{2\gamma_t(\gamma_t+2)}{\gamma_{\rm RD}}\right). \end{aligned} \tag{40}$$

Similarly, we can obtain the probability of satisfying the channel condition of successful transmission in the UL-NOMA mode for $|g_{\rm main}|^2 \leq |g_{\rm sub}|^2$ as follows:

$$\begin{aligned} P_{\mathcal{D}_{\rm UL}^2} &= \int_{\frac{\gamma_t(\gamma_t+2)}{\gamma_{\rm RD}}}^{\infty} \exp\left(-\frac{x^2\gamma_{\rm RD} - x{\gamma_t}^2}{x\gamma_{\rm RD}-\gamma_t(\gamma_t+1)}\right){\rm d}x \\ &\quad - \frac{1}{2}\exp\left(-\frac{2\gamma_t(\gamma_t+2)}{\gamma_{\rm RD}}\right). \end{aligned} \tag{41}$$

Fig. 5 illustrates the areas $\mathcal{D}_{\rm UL}^1$ and $\mathcal{D}_{\rm UL}^2$, which correspond to the successful transmissions in our UL-NOMA mode under the assumptions of $|g_{\rm main}|^2 \geq |g_{\rm sub}|^2$ and $|g_{\rm main}|^2 \leq |g_{\rm sub}|^2$, respectively.

3) Unicast Modes for the SR Transmission and RD Relaying Phases: In the unicast modes for the SR transmission and RD relaying phases, a single packet is transmitted. From (19) and (21), the probability corresponding to the channel condition required for successful transmission in the SR transmission phase and that of the RD relaying phase are given, respectively, by [25]

$$P_{\rm uni}^{\rm SR} = \int_{\frac{\gamma_t}{\gamma_{\rm SR}}}^{\infty} e^{-x}{\rm d}x = e^{-\frac{\gamma_t}{\gamma_{\rm SR}}} \tag{42}$$

$$P_{\rm uni}^{\rm RD} = \int_{\frac{\gamma_t}{\gamma_{\rm RD}}}^{\infty} e^{-x}{\rm d}x = e^{-\frac{\gamma_t}{\gamma_{\rm RD}}}. \tag{43}$$

4) Broadcast Mode for the SR Transmission Phase: In the broadcast mode for the SR transmission phase, both of the two SR links have to be activated in a simultaneous manner. Hence, the probability of the channel condition imposed by the successful transmission is the square of that of the unicast mode, which is represented by

$$P_{\rm broad} = \left(P_{\rm uni}^{\rm SR}\right)^2 \tag{44}$$

$$= e^{-\frac{2\gamma_t}{\gamma_{\rm SR}}}. \tag{45}$$

B. Theoretical Outage Probability and Throughput

First, we derive the state transition matrix defined by $\mathbf{A} \in \mathcal{R}^{N_{\rm state}\times N_{\rm state}}$, where $N_{\rm state}$ denotes the number of legitimate states. Additionally, the pth-row qth-column element of $\mathbf{A}$ indicates the transition probability from state s_q to state s_p, which is represented by ${\rm A}_{pq}$. Moreover, given the current state s_q, $\Xi_1^{(q)}, \ldots, \Xi_{N_q}^{(q)}$ are a set of transitions, where N_q represents the number of potential transitions. Furthermore, $\Xi_1^{(q)}, \ldots, \Xi_{N_q}^{(q)}$ are ordered based on the priority defined in our algorithms, shown in Tables II and III, where $\Xi_1^{(q)}$ corresponds to the highest priority in the mode selection. Let us define $s_{f(\Xi_i^{(q)})}$ as the state reached from state s_q with the transition $\Xi_i^{(q)}$. Then, the transition probability ${\rm A}_{f(\Xi_i^{(q)})q}$ from state s_q to state $s_{f(\Xi_i^{(q)})}$ is given by

$${\rm A}_{f(\Xi_i^{(q)})q} = \Pr\left(\overline{\Xi}_1^{(q)} \cap \ldots \cap \overline{\Xi}_{i-1}^{(q)} \cap \Xi_i^{(q)}\right), \tag{46}$$

where the transition $\Xi_i^{(q)}$ is successful, while all other transitions with higher priorities than $\Xi_i^{(q)}$ are in outage. Furthermore, the outage probability under state s_q is expressed as

$$P_{\rm out}^{s_q} = {\rm A}_{qq} = \Pr\left(\overline{\Xi}_1^{(q)} \cap \cdots \cap \overline{\Xi}_{N_q}^{(q)}\right). \tag{47}$$

In order to exemplify calculation of outage probability (47), let us consider that the state shown in Fig. 3 is state s_q, where the first relay and the second relay nodes have two and one packets, which are all different. In this case, there are $N_q = 7$ potential states which can be potentially transitioned to from state s_q, as listed in Table IV. The symbols $\triangle$, $\Diamond$, $\square$, $\bigcirc$, and $\heartsuit$ denote five different packets. Then, the $N_q = 7$ transition probabilities are calculated as

$${\rm A}_{f(\Xi_1^{(q)})q} = \Pr\left(\Xi_1^{(q)}\right) = P_{\mathcal{D}_{\rm DL}^1} + P_{\mathcal{D}_{\rm DL}^2} \tag{48}$$

$$\begin{aligned} {\rm A}_{f(\Xi_2^{(q)})q} &= \Pr\left(\overline{\Xi}_1^{(q)} \cap \Xi_2^{(q)}\right) = \Pr\left(\Xi_2^{(q)}\right) - \Pr\left(\Xi_1^{(q)}\right) \\ &= P_{\rm broad} - \left(P_{\mathcal{D}_{\rm DL}^1} + P_{\mathcal{D}_{\rm DL}^2}\right) \end{aligned} \tag{49}$$

$$\begin{aligned} {\rm A}_{f(\Xi_3^{(q)})q} &= \Pr\left(\overline{\Xi}_1^{(q)} \cap \overline{\Xi}_2^{(q)} \cap \Xi_3^{(q)}\right) \\ &= \Pr\left(\Xi_3^{(q)}\right) - \Pr\left(\Xi_1^{(q)} \cup \Xi_2^{(q)}\right) \\ &= P_{\rm uni}^{\rm SR} - P_{\rm broad} \end{aligned} \tag{50}$$

TABLE IV
STATES TRANSITIONED TO FROM THE STATE OF FIG. 3

States	main-link	active mode	Relay 1				Relay 2			
$s_{f(\Xi_1)}$	SR_2	DL-NOMA mode	△	◇	□	empty	◯	□	♡	empty
$s_{f(\Xi_2)}$	SR_2	Broadcast mode	△	◇	□	empty	◯	□	empty	empty
$s_{f(\Xi_3)}$	SR_2	Unicast mode	△	◇	empty	empty	◯	□	empty	empty
$s_{f(\Xi_4)}$	$\mathrm{R}_1\mathrm{D}$	UL-NOMA mode	△	empty	empty	empty	empty	empty	empty	empty
$s_{f(\Xi_5)}$	$\mathrm{R}_1\mathrm{D}$	Unicast mode	△	empty	empty	empty	◯	empty	empty	empty
$s_{f(\Xi_6)}$	SR_1	Unicast mode	△	◇	□	empty	◯	empty	empty	empty
$s_{f(\Xi_7)}$	$\mathrm{R}_2\mathrm{D}$	Unicast mode	△	◇	empty	empty	empty	empty	empty	empty

$$\begin{aligned}\mathrm{A}_{f(\Xi_4^{(q)})q} &= \Pr\left(\overline{\Xi}_1^{(q)} \cap \overline{\Xi}_2^{(q)} \cap \overline{\Xi}_3^{(q)} \cap \Xi_4^{(q)}\right)\\ &= \left\{1 - \Pr\left(\Xi_1^{(q)} \cup \Xi_2^{(q)} \cup \Xi_3^{(q)}\right)\right\}\\ &\quad \times \Pr\left(\Xi_4^{(q)}\right)\\ &= \left(1 - P_{\mathrm{uni}}^{\mathrm{SR}}\right)\left(P_{\mathcal{D}_{\mathrm{UL}}^1} + P_{\mathcal{D}_{\mathrm{UL}}^2}\right) \qquad (51)\\ \mathrm{A}_{f(\Xi_5^{(q)})q} &= \Pr\left(\overline{\Xi}_1^{(q)} \cap \overline{\Xi}_2^{(q)} \cap \overline{\Xi}_3^{(q)} \cap \overline{\Xi}_4^{(q)} \cap \Xi_5^{(q)}\right)\\ &= \left\{1 - \Pr\left(\Xi_1^{(q)} \cup \Xi_2^{(q)} \cup \Xi_3^{(q)}\right)\right\}\\ &\quad \times \{\Pr(\Xi_5) - \Pr(\Xi_4)\}\\ &= \left(1 - P_{\mathrm{uni}}^{\mathrm{SR}}\right)\left\{P_{\mathrm{uni}}^{\mathrm{RD}} - \left(P_{\mathcal{D}_{\mathrm{UL}}^1} + P_{\mathcal{D}_{\mathrm{UL}}^2}\right)\right\} \qquad (52)\\ \mathrm{A}_{f(\Xi_6^{(q)})q} &= \Pr\left(\overline{\Xi}_1^{(q)} \cap \overline{\Xi}_2^{(q)} \cap \overline{\Xi}_3^{(q)} \cap \overline{\Xi}_4^{(q)} \cap \overline{\Xi}_5^{(q)} \cap \Xi_6^{(q)}\right)\\ &= \left\{1 - \Pr\left(\Xi_1^{(q)} \cup \Xi_2^{(q)} \cup \Xi_3^{(q)}\right)\right\}\\ &\quad \times \left\{1 - \Pr\left(\Xi_4^{(q)} \cup \Xi_5^{(q)}\right)\right\}\Pr\left(\Xi_6^{(q)}\right)\\ &= \left(1 - P_{\mathrm{uni}}^{\mathrm{SR}}\right)\left(1 - P_{\mathrm{uni}}^{\mathrm{RD}}\right)P_{\mathrm{uni}}^{\mathrm{SR}} \qquad (53)\\ \mathrm{A}_{f(\Xi_7^{(q)})q} &= \Pr\left(\overline{\Xi}_1^{(q)} \cap \overline{\Xi}_2^{(q)} \cap \overline{\Xi}_3^{(q)} \cap \overline{\Xi}_4^{(q)} \cap \overline{\Xi}_5^{(q)}\right.\\ &\qquad \left.\cap \overline{\Xi}_6^{(q)} \cap \Xi_7^{(q)}\right)\\ &= \left\{1 - \Pr\left(\Xi_1^{(q)} \cup \Xi_2^{(q)} \cup \Xi_3^{(q)}\right)\right\}\\ &\quad \times \left\{1 - \Pr\left(\Xi_4^{(q)} \cup \Xi_5^{(q)}\right)\right\}\\ &\quad \times \left\{1 - \Pr\left(\Xi_6^{(q)}\right)\right\}\Pr\left(\Xi_7^{(q)}\right)\\ &= \left(1 - P_{\mathrm{uni}}^{\mathrm{SR}}\right)^2\left(1 - P_{\mathrm{uni}}^{\mathrm{RD}}\right)P_{\mathrm{uni}}^{\mathrm{RD}}. \qquad (54)\end{aligned}$$

Moreover, the outage probability under state s_q of this specific example is given by

$$\begin{aligned}P_{\mathrm{out}}^{s_q} &= \mathrm{A}_{qq}\\ &= \Pr\left(\overline{\Xi}_1^{(q)} \cap \overline{\Xi}_2^{(q)} \cap \overline{\Xi}_3^{(q)} \cap \overline{\Xi}_4^{(q)} \cap \overline{\Xi}_5^{(q)} \cap \overline{\Xi}_6^{(q)} \cap \overline{\Xi}_7^{(q)}\right)\\ &= \left\{1 - \Pr\left(\Xi_1^{(q)} \cup \Xi_2^{(q)} \cup \Xi_3^{(q)}\right)\right\}\\ &\quad \times \left\{1 - \Pr\left(\Xi_4^{(q)} \cup \Xi_5^{(q)}\right)\right\}\\ &\quad \times \left\{1 - \Pr\left(\Xi_6^{(q)}\right)\right\}\left\{1 - \Pr\left(\Xi_7^{(q)}\right)\right\}\\ &= \left(1 - P_{\mathrm{uni}}^{\mathrm{SR}}\right)^2\left(1 - P_{\mathrm{uni}}^{\mathrm{RD}}\right)^2. \qquad (55)\end{aligned}$$

The steady-state probabilities $\boldsymbol{\pi} = [\pi_1, \ldots, \pi_{N_{\mathrm{state}}}]^T \in \mathcal{R}^{N_{\mathrm{state}}}$ are formulated as [34]

$$\boldsymbol{\pi} = (\mathbf{A} - \mathbf{I} + \mathbf{B})^{-1}\mathbf{b}, \qquad (56)$$

where all the elements in the matrix $\mathbf{B} \in \mathcal{R}^{N_{\mathrm{state}} \times N_{\mathrm{state}}}$ and the vector $\mathbf{b} \in \mathcal{R}^{N_{\mathrm{state}}}$ are ones. Since the qth diagonal element of $\mathbf{A}$, i.e., A_{qq}, represents the outage probability of the state s_q, we have the average outage probability

$$\begin{aligned}P_{\mathrm{out}} &= \sum_{q=1}^{N_{\mathrm{state}}} \mathrm{A}_{qq}\pi_q \qquad (57)\\ &= \mathrm{diag}(\mathbf{A})\boldsymbol{\pi}. \qquad (58)\end{aligned}$$

Also, the theoretical throughput is formulated by

$$\eta = \sum_{q=1}^{N_{\mathrm{state}}} \pi_q \left(\sum_{i=1}^{N_q} \mathrm{A}_{f(\Xi_i^{(q)})q} \cdot \varepsilon_{f(\Xi_i^{(q)})q}\right), \qquad (59)$$

where $\varepsilon_{f(\Xi_i^{(q)})q}$ is the number of different packets transmitted in the selected mode transitioned from state q to state $s_{f(\Xi_i^{(q)})}$.

C. Theoretical Average Packet Delay

Based on Little's law [35], the average packet delay at node t is given by

$$\mathbb{E}[D_t] = \frac{\mathbb{E}[\Psi_t]}{\eta_t}, \qquad (60)$$

where $\mathbb{E}[\Psi_t]$ denotes the average queuing length and η_t denotes the throughput at node t. The average packet delay consists of the delay at the source node and that at the relay nodes, which are represented by $\mathbb{E}[D_S]$ and $\mathbb{E}[D_R]$, respectively. Similar to previous studies [27], [29], $\eta_S = \mathbb{E}[\Psi_S]$ and so $\mathbb{E}[D_S] = 1$. On the other hand, since our proposed scheme assumes a two-hop network, and if the source node transmits a sufficiently high number of packets, it can be considered that the transitions on the SR links and RD links are selected with almost equal probability, the system's average throughput is the value obtained in (59) multiplied by 1/2. Moreover, we assume two relay nodes and they have the same probability of being chosen, so we have

$$\eta_R = \frac{\eta}{2 \times 2}. \qquad (61)$$

Furthermore, the average queuing length of the relay nodes is given by

$$\mathbb{E}[\Psi_R] = \frac{1}{2}\sum_{i=1}^{N_{\text{state}}} \pi_i \Psi(i), \tag{62}$$

where $\Psi(i)$ denotes the number of different packets stored at the relay nodes in state s_i. Therefore, the average packet delay of the relay nodes is

$$\mathbb{E}[D_R] = \frac{\mathbb{E}[\Psi_R]}{\eta_R} = \frac{2}{\eta}\sum_{i=1}^{N_{\text{state}}} \pi_i \Psi(i), \tag{63}$$

from which we obtain the average packet delay of the system, represented as

$$\mathbb{E}[D] = \mathbb{E}[D_S] + \mathbb{E}[D_R] = 1 + \frac{2}{\eta}\sum_{i=1}^{N_{\text{state}}} \pi_i \Psi(i). \tag{64}$$

D. Theoretical Diversity Order

In order to derive the theoretical achievable diversity order of the proposed scheme, we assume that all the SR and RD links are independent and identically distributed. The diversity order is defined by [35]

$$\mathcal{D} = -\lim_{\overline{\gamma}\to\infty} \frac{\log P_{\text{out}}}{\log \overline{\gamma}}, \tag{65}$$

where we have the average SNR of $\gamma_{\text{SR}} = \gamma_{\text{RD}} = \overline{\gamma}$. In the limit of $\overline{\gamma} \to \infty$, channel capacities of all the links are higher than the target rate in each mode, and hence transmission is successful. Therefore, the number of packets stored at each relay node's buffer is maintained to be $\xi_{\text{SR}} \le \Phi_k \le \xi_{\text{RD}} (k = 1, 2)$, where the buffer state is neither empty nor full, except for the special case of $(\xi_{\text{SR}}, \xi_{\text{RD}}) = (1, 2)$ and $L = 3$. Moreover, if both the unicast transmission modes in the SR transmission and the RD relaying phases are in the outage, the four other transmission modes are naturally in the outage. This implies that P_{out} only depends on the outage probabilities of the two unicast modes. Hence, except for the case of $(\xi_{\text{SR}}, \xi_{\text{RD}}) = (1, 2)$ and $L = 3$, the achievable maximum diversity order of the proposed scheme (65) is modified to

$$\mathcal{D} = -\lim_{\overline{\gamma}\to\infty} \frac{\log\left(1 - P_{\text{uni}}^{\text{SR}}\right)^2 \left(1 - P_{\text{uni}}^{\text{RD}}\right)^2}{\log \overline{\gamma}} \tag{66}$$

$$\approx -\lim_{\overline{\gamma}\to\infty} \frac{\log\left(\frac{\gamma_t}{\overline{\gamma}}\right)^4}{\log \overline{\gamma}}$$

$$= 4 \tag{67}$$

where from (66) to (67) we used the relationship of $\mathrm{e}^x \approx 1 + x$, which is valid for the limit of $x \to 0$.

V. Simulation Results

In this section, we provide our simulation results as an evaluation of the performance of the proposed scheme, comparing these with those of the two conventional buffer-state-based (BSB) protocols, which are the original BSB [18] and the BBSB protocols [27], selected as benchmark schemes. We assumed that the transmission rate of each node is fixed as $r_0 = 1$ bps/Hz. This implies that by adapting the transmission power to be minimum while maintaining the transmission to be successful, energy-efficient transmission is possible. Moreover, we assumed that the buffers of all nodes are initially empty and a sufficient number of packets are transmitted to attain the steady state in each Monte Carlo simulation, as verified in [27]. Also, unless otherwise stated, we set the average SNRs to be identical, $\gamma_{\text{SR}} = \gamma_{\text{RD}}$, whereas the threshold parameters are set as $\xi_{\text{SR}} = 1$ and $\xi_{\text{RD}} = 2$.

First, in Fig. 6, in order to validate our system model, we compare the theoretical bounds of the proposed scheme derived in Section IV and the numerical results, where the buffer size was set to $L = 3$. Note that only in this result, the cooperative beamforming mode is deactivated. Figs. 6(a), 6(b), and 6(c) show the throughput, outage probability, and packet delay, respectively; as shown, it was found that the numerical and theoretical curves matched well. Hence, the system model of the proposed scheme was validated.

Next, Fig. 7 shows the numerical throughput for the proposed scheme with and without cooperative beamforming, the BSB scheme, and the BBSB scheme, where the buffer size was set to $L = 5$ and the average SNR was varied from $\gamma = 0$ to 20 dB. Observe in Fig. 7 that the proposed scheme with and without cooperative beamforming achieved the highest throughput among the four schemes in the entire SNR regime. Moreover, in this specific scenario, the proposed scheme with and without cooperative beamforming showed almost the same performance. The benefits of the proposed schemes over the benchmark schemes were remarkable, especially at high SNRs. This was achieved as the explicit benefit of the inclusion of the two NOMA modes in the proposed schemes.

Furthermore, Fig. 8 shows the average packet delays of the four schemes with a buffer size of $L = 5$ and the average SNR varied from $\gamma = 0$ to 20 dB. As shown in Fig. 8, it was found that the proposed schemes with and without cooperative beamforming exhibited nearly the same performance, and both outperformed the two latest benchmark schemes. The proposed scheme's performance advantages increased upon increasing the average SNR. Further investigations of the effects of the threshold parameters are given later in this Section.

In Fig. 9, we considered scenarios of asymmetric channels, i.e., those of $\gamma_{\text{SR}} \neq \gamma_{\text{RD}}$. More specifically, Figs. 9(a) and 9(b) show the throughput and the average packet delay of the proposed schemes with and without cooperative beamforming, the BSB scheme [18], and the GBSB scheme [27], respectively. The buffer size was set to $L = 5$, and the average SNR of the RD links was fixed as $\gamma_{\text{RD}} = 5$ dB. Observe in Fig. 9 that the proposed scheme with cooperative beamforming achieved better performance than that without cooperative beamforming in terms of both the throughput and the packet delay. Furthermore, it is seen that the cooperative beamforming gain improved upon increasing the average SNR of the SR links γ_{SR}. This is because, in such a scenario, the number of shared packets among the relay nodes tend to be higher, hence having a high possibility of the activation of the cooperative beamforming

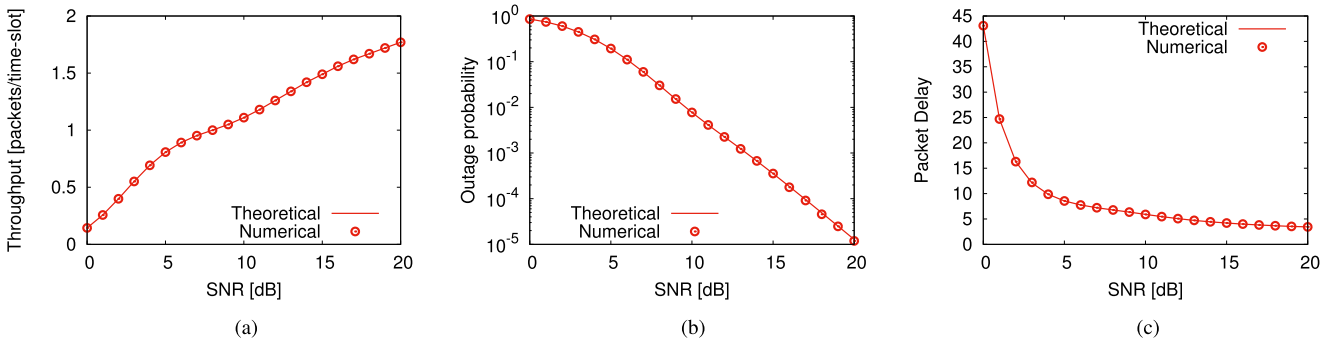

Fig. 6. Numerical and theoretical results of proposed scheme without cooperative beamforming mode for (a) throughput and (b) packet delay with buffer size $L = 3$ and the average SNR γ varied from 0 to 20 dB. (a) Throughput. (b) Outage probability. (c) Average packet delay.

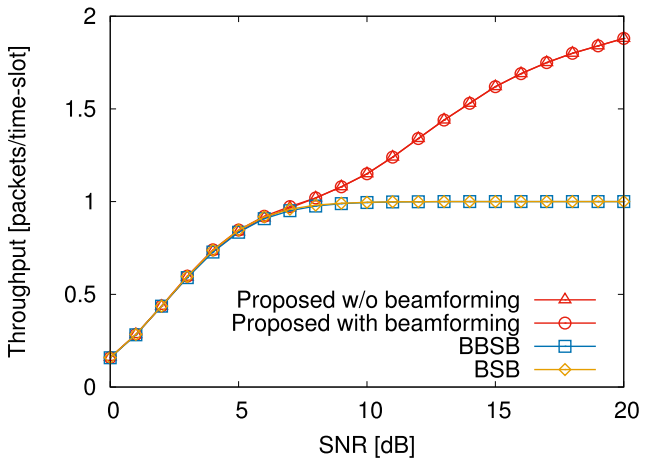

Fig. 7. Numerical throughput of the proposed scheme with and without cooperative beamforming, the BSB scheme [18], and the BBSB scheme [27] with buffer size $L = 5$ and average SNR varied from $\gamma = 0$ to 20 dB.

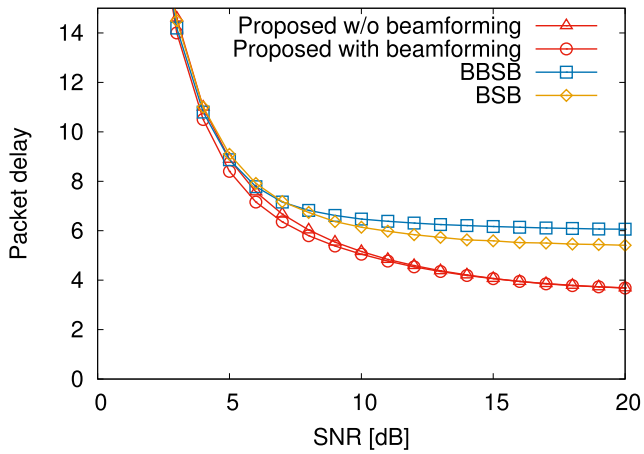

Fig. 8. Average packet delay of the proposed schemes with and without cooperative beamforming, the BSB scheme [18], and the GBSB scheme [27] with buffer size $L = 5$ and average SNR varied from $\gamma = 0$ to 20 dB.

mode in the low SNR regime of the RD links γ_{RD}. Also in this figure, although the proposed schemes outperformed the two latest benchmark schemes in terms of throughput, the performance of proposed schemes were below in some SNRs for packet delay. This is likely because that the DL-NOMA mode causes more packets to be sent form the source node and increases the number of packets held in the buffer of the relay nodes.

Additionally, Fig. 10 shows the distribution of selected mode in the proposed scheme with beamforming, where the buffer size was $L = 5$ and the average SNR was varied from $\gamma = 0$ to 20 dB. Observe in Fig. 10 that in the low SNR regime, two unicast modes and the outage event are dominant, as expected. Upon increasing the SNR value, the ratios of the two NOMA modes increased. This allows us to achieve increased throughput, as shown in Fig. 7.

Finally, we investigated the effects of the threshold parameters ξ_{SR} and ξ_{RD} on the achievable performance of the proposed schemes. In the proposed schemes, by changing these threshold parameters, the tradeoff between the throughput, the average packet delay, and the outage probability are balanced. Hence, depending on the cost function targeted, the optimal ξ_{SR} and ξ_{RD} values change. Figs. 11, 12, and 13 show the achievable performance of the throughput, the average packet delay, and the outage probability of the proposed scheme with beamforming for a buffer size of $L = 5$ and average SNR varied from $\gamma = 0$ to 20 dB. The examined pairs of threshold parameters were $(\xi_{\mathrm{SR}}, \xi_{\mathrm{RD}}) = (1,2), (1,3), (1,4), (2,3), (2,4)$, and (3,4). Observe in Fig. 11 that almost the same throughput was exhibited regardless of the threshold parameters except in the case of $(\xi_{\mathrm{SR}}, \xi_{\mathrm{RD}}) = (3,4)$. As shown in Fig. 12, it was found that the average packet delay of $(\xi_{\mathrm{SR}}, \xi_{\mathrm{RD}}) = (1,2)$ achieved the best performance, followed by that of $(\xi_{\mathrm{SR}}, \xi_{\mathrm{RD}}) = (1,3)$. This is because, as shown in (64), the average packet delay decreases upon decreasing the number of packets stored in the buffers of the relay nodes. Fig. 13 shows that the outage probability of $(\xi_{\mathrm{SR}}, \xi_{\mathrm{RD}}) = (2,3)$ achieved the best performance, followed by that of $(\xi_{\mathrm{SR}}, \xi_{\mathrm{RD}}) = (1,3)$. Therefore, the appropriate $(\xi_{\mathrm{SR}}, \xi_{\mathrm{RD}})$ set should be selected depending on the target system requirement, according to the simulated results.

To provide further insight, an additional mode based on virtual full-duplex transmission [36] may be incorporated into our scheme. In this mode, while source node transmits an information packet to a relay node, another relay node transmits a

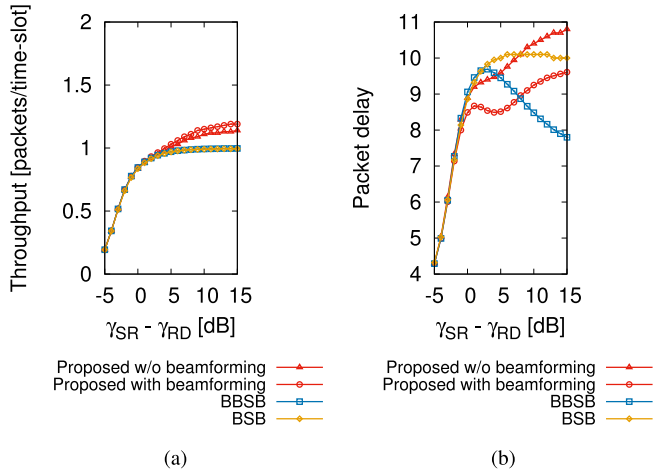

Fig. 9. Throughput and average packet delay of the proposed schemes with and without cooperative beamforming in the asymmetric channels with buffer size $L = 5$ and average SNR of RD links fixed as $\gamma_{\mathrm{RD}} = 5$ dB. (a) Throughput. (b) Average packet delay.

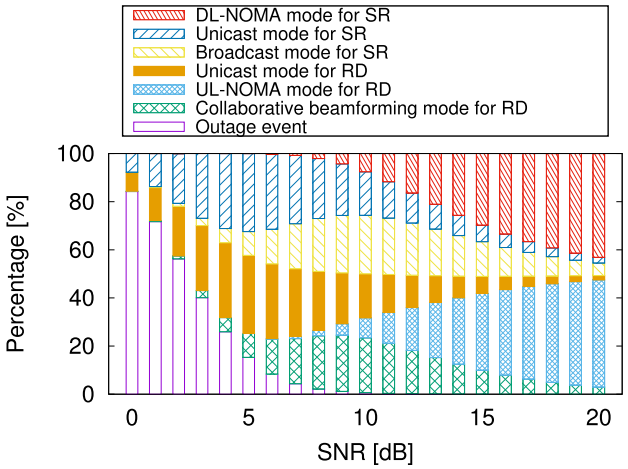

Fig. 10. Distribution of the selected mode in our proposed scheme with beamforming with buffer size $L = 5$ and average SNR varied from $\gamma = 0$ to 20 dB.

buffered packet to a destination node, and hence the transmission rate may be increased. However, the incorporation of this mode into our scheme is the scope of this paper, which is left for future studies.

In this paper, we focused our attention on the single-source and single-destination scenario with two relay nodes. However, the proposed scheme can be readily extended to the scenarios supporting more than two relay nodes. More specifically, the four OMA modes in our scheme can be used for more than three relay nodes similar to [27], while the two NOMA modes, i.e., the UL- and DL-NOMA modes, are originally developed for supporting more than two nodes. Alternatively, it may be practical to select appropriate two out of multiple relay nodes in order to support the arbitrary number of relay nodes in our scheme. Furthermore, the proposed scheme is also applicable to

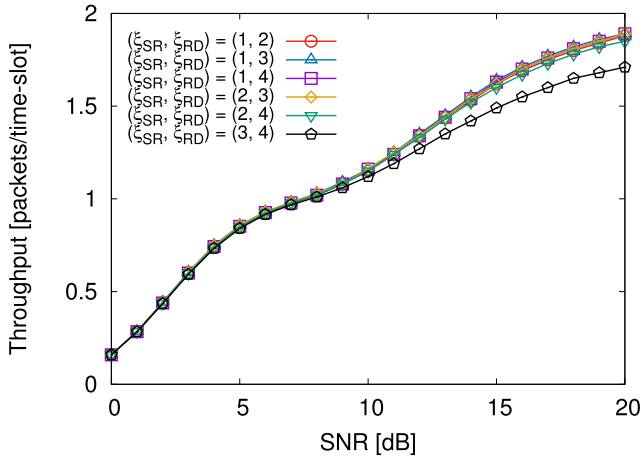

Fig. 11. Effects of the threshold parameters of the proposed scheme with beamforming on the throughput. We considered a buffer size of $L = 5$ and varied the average SNR from $\gamma = 0$ to 20 dB.

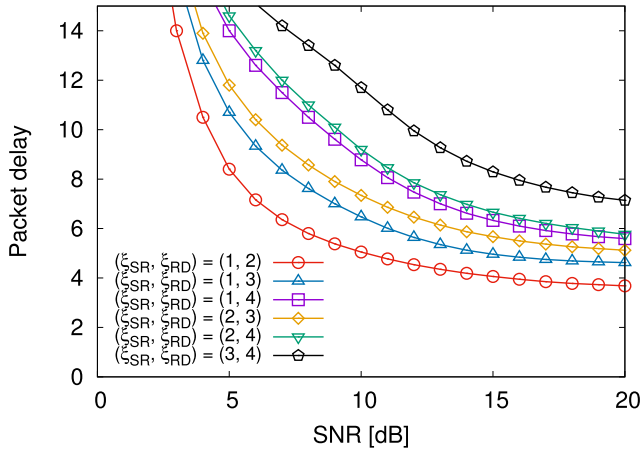

Fig. 12. Effects of the threshold parameters of the proposed scheme with beamforming on the average packet delay. We considered a buffer size of $L = 5$ and varied the average SNR from $\gamma = 0$ to 20 dB.

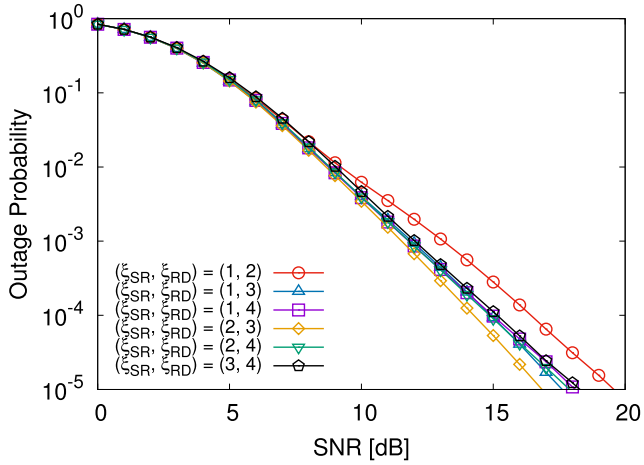

Fig. 13. Effects of the threshold parameters of the proposed scheme with beamforming on the outage probability. We considered a buffer size of $L = 5$ and varied the average SNR from $\gamma = 0$ to 20 dB.

multi-user scenarios by relying on the existing medium access control (MAC) protocols, such as time-division multiple access, frequency-domain multiple access, and carrier-sense multiple access.

VI. Conclusion

In this paper, we proposed novel NOMA/OMA-hybrid multi-mode buffer-state-based cooperative schemes. More specifically, our DL-NOMA mode and broadcast mode allows multiple relay nodes to store different and same packets, respectively. Also, the UL-NOMA mode and the cooperative beamforming mode become possible owing to the packets shared among the relay nodes. The theoretical bounds of the throughput, the average packet delay, and the outage probability were derived for the proposed scheme without cooperative beamforming. Our simulation results demonstrated that the appropriate switching of the six modes in the proposed scheme allows us to achieve nearly doubled throughput and reduced average packet delay in the high SNR regime in comparison to the conventional BSB and BBSB schemes.

References

[1] Y. Saito, Y. Kishiyama, A. Benjebbour, T. Nakamura, A. Li, and K. Higuchi, "Non-orthogonal multiple access (NOMA) for cellular future radio access," in *Proc. IEEE 77th Veh. Technol. Conf.*, Dresden, Germany, Jun. 2013, pp. 1–5.

[2] Z. Ding, X. Lei, G. K. Karagiannidis, R. Schober, J. Yuan, and V. K. Bhargava, "A survey on non-orthogonal multiple access for 5G networks: Research challenges and future trends," *IEEE J. Sel. Areas Commun.*, vol. 35, no. 10, pp. 2181–2195, Oct. 2017.

[3] Y. Liu, Z. Qin, M. Elkashlan, Z. Ding, A. Nallanathan, and L. Hanzo, "Nonorthogonal multiple access for 5G and beyond," *Proc. IEEE* vol. 105, no. 12, pp. 2347–2381, Dec. 2017.

[4] L. Lv, J. Chen, Q. Ni, and Z. Ding, "Design of cooperative non-orthogonal multicast cognitive multiple access for 5G systems: User scheduling and performance analysis," *IEEE Trans. Commun.*, vol. 65, no. 6, pp. 2641–2656, Jun. 2017.

[5] L. Lv, J. Chen, Q. Ni, Z. Ding, and H. Jiang, "Cognitive non-orthogonal multiple access with cooperative relaying: A. new wireless frontier for 5G spectrum sharing," *IEEE Commun. Mag.*, vol. 56, no. 4, pp. 188–195, Apr. 2018.

[6] H. V. Cheng, E. Bjornson, and E. G. Larsson, "Performance analysis of NOMA in training-based multiuser MIMO systems," *IEEE Trans. Wireless Commun.*, vol. 17, no. 1, pp. 372–385, Jan. 2018.

[7] K. Senel, H. V. Cheng, E. Bjornson, and E. G. Larsson, "What role can NOMA play in massive MIMO?," *IEEE J. Sel. Top. Signal Process.*, vol. 13, no. 3, pp. 597–611, Jun. 2019.

[8] M. Bashar, K. Cumanan, A. G. Burr, H. Q. Ngo, L. Hanzo, and P. Xiao, "On the performance of cell-free massive MIMO relying on adaptive NOMA/OMA mode-switching," *IEEE Trans. Commun.*, vol. 68, no. 2, pp. 792–810, Feb. 2020.

[9] Z. Yang, Z. Ding, P. Fan, and N. Al-Dhahir, "A general power allocation scheme to guarantee quality of service in downlink and uplink NOMA systems," *IEEE Trans. Wireless Commun.*, vol. 15, no. 11, pp. 7244–7257, Nov. 2016.

[10] M. A. Sedaghat and R. R. Muller, "On user pairing in uplink NOMA," *IEEE Trans. Wireless Commun.*, vol. 17, no. 5, pp. 3474–3486, May 2018.

[11] A. Nosratinia, T. E. Hunter, and A. Hedayat, "Cooperative communication in wireless networks," *IEEE Commun. Mag.*, vol. 42, no. 10, pp. 74–80, Oct. 2004.

[12] A. Bletsas, A. Khisti, D. P. Reed, and A. Lippman, "A simple cooperative diversity method based on network path selection," *IEEE J. Sel. Areas Commun.*, vol. 24, no. 3, pp. 659–672, Mar. 2006.

[13] S. Sugiura, S. Chen, H. Haas, P. M. Grant, and L. Hanzo, "Coherent versus non-coherent decode-and-forward relaying aided cooperative space-time shift keying," *IEEE Trans. Commun.*, vol. 59, no. 6, pp. 1707–1719, Jun. 2011.

[14] S. Sugiura, S. X. Ng, L. Kong, S. Chen, and L. Hanzo, "Quasi-synchronous cooperative networks: A. practical cooperative transmission protocol," *IEEE Veh. Technol. Mag.*, vol. 7, no. 4, pp. 66–76, Dec. 2012.

[15] N. B. Mehta, V. Sharma, and G. Bansal, "Performance analysis of a cooperative system with rateless codes and buffered relays," *IEEE Trans. Wireless Commun.*, vol. 10, no. 4, pp. 1069–1081, Apr. 2011.

[16] A. Ikhlef, J. Kim, and R. Schober, "Mimicking full-duplex relaying using half-duplex relays with buffers," *IEEE Trans. Veh. Technol.*, vol. 61, no. 7, pp. 3025–3037, Sep. 2012.

[17] I. Ahmed, A. Ikhlef, R. Schober, and R. K. Mallik, "Power allocation for conventional and buffer-aided link adaptive relaying systems with energy harvesting nodes," *IEEE Trans. Wireless Commun.*, vol. 13, no. 3, pp. 1182–1195, Mar. 2014.

[18] S. Luo and K. Teh, "Buffer state based relay selection for buffer-aided cooperative relaying systems," *IEEE Trans. Wireless Commun.*, vol. 14, no. 10, pp. 5430–5439, Oct. 2015.

[19] M. Oiwa, C. Tosa, and S. Sugiura, "Theoretical analysis of hybrid buffer-aided cooperative protocol based on max-max and max-link relay selections," *IEEE Trans. Veh. Technol.*, vol. 65, no. 11, pp. 9236–9246, Nov. 2016.

[20] N. Nomikos, T. Charalambous, D. Vouyioukas, and G. K. Karagiannidis, "Low-complexity buffer-aided link selection with outdated CSI and feedback errors," *IEEE Trans. Commun.*, vol. 66, no. 8, pp. 3694–3706, Aug. 2018.

[21] S. Luo and K. C. Teh, "Adaptive transmission for cooperative NOMA system with buffer-aided relaying," *IEEE Commun. Lett.*, vol. 21, no. 4, pp. 937–940, Apr. 2017.

[22] P. Xu, J. Quan, Z. Yang, G. Chen, and Z. Ding, "Performance analysis of buffer-aided hybrid NOMA/OMA in cooperative uplink system," *IEEE Access*, vol. 7, pp. 168 759–168 773, 2019.

[23] M. Alkhawatrah, Y. Gong, G. Chen, S. Lambotharan, and J. A. Chambers, "Buffer-aided relay selection for cooperative NOMA in the internet of things," *IEEE Internet Things J.*, vol. 6, no. 3, pp. 5722–5731, Jun. 2019.

[24] N. Nomikos, T. Charalambous, D. Vouyioukas, G. K. Karagiannidis, and R. Wichman, "Hybrid NOMA/OMA with buffer-aided relay selection in cooperative networks," *IEEE J. Sel. Top. Signal Process.*, vol. 13, no. 3, pp. 524–537, Jun. 2019.

[25] M. Oiwa and S. Sugiura, "Reduced-packet-delay generalized buffer-aided relaying protocol: Simultaneous activation of multiple source-to-relay links," *IEEE Access*, vol. 4, pp. 3632–3646, 2016.

[26] M. Oiwa, R. Nakai, and S. Sugiura, "Buffer-state-and-thresholding-based amplify-and-forward cooperative networks," *IEEE Wireless Commun. Lett.*, vol. 6, no. 5, pp. 674–677, Oct. 2017.

[27] R. Nakai, M. Oiwa, K. Lee, and S. Sugiura, "Generalized buffer-state-based relay selection with collaborative beamforming," *IEEE Trans. Veh. Technol.*, vol. 67, no. 2, pp. 1245–1257, Feb. 2018.

[28] R. Nakai and S. Sugiura, "Physical layer security in buffer-state-based max-ratio relay selection exploiting broadcasting with cooperative beamforming and jamming," *IEEE Trans. Inf. Forensics Secur.*, vol. 14, no. 2, pp. 431–444, Feb. 2019.

[29] J. Kochi, R. Nakai, and S. Sugiura, "Performance evaluation of generalized buffer-state-based relay selection in NOMA-aided downlink," *IEEE Access*, vol. 7, pp. 173 320–173 328, 2019.

[30] R. Zhang, R. Nakai, K. Sezaki, and S. Sugiura, "Generalized buffer-state-based relay selection in cooperative cognitive radio networks," *IEEE Access*, vol. 8, pp. 11 644–11 657, 2020.

[31] Z. Yang, Z. Ding, P. Fan, and N. Al-Dhahir, "A general power allocation scheme to guarantee quality of service in downlink and uplink NOMA systems," *IEEE Trans. Wireless Commun.*, vol. 15, no. 11, pp. 7244–7257, Nov. 2016.

[32] M. F. Kader, M. B. Shahab, and S. Y. Shin, "Exploiting non-orthogonal multiple access in cooperative relay sharing," *IEEE Commun. Lett.*, vol. 21, no. 5, pp. 1159–1162, May 2017.

[33] M. S. Ali, H. Tabassum, and E. Hossain, "Dynamic user clustering and power allocation for uplink and downlink non-orthogonal multiple access (NOMA) systems," *IEEE Access*, vol. 4, pp. 6325–6343, 2016.

[34] I. Krikidis, T. Charalambous, and J. S. Thompson, "Buffer-aided relay selection for cooperative diversity systems without delay constraints," *IEEE Trans. Wireless Commun.*, vol. 11, no. 5, pp. 1957–1967, May 2012.

[35] Z. Tian, G. Chen, Y. Gong, Z. Chen, and J. A. Chambers, "Buffer-aided max-link relay selection in amplify-and-forward cooperative networks," *IEEE Trans. Veh. Technol.*, vol. 64, no. 2, pp. 553–565, Feb. 2015.

[36] T. Mishina, M. Oiwa, R. Nakai, and S. Sugiura, "Buffer-aided virtual full-duplex cooperative networks exploiting source-to-relay broadcast channels," in *Proc. IEEE Veh. Technol. Conf.*, Honolulu, HI, USA, Sep. 2019, pp. 1–5.

Jun Kochi received the B.E. degree in computer and information sciences in 2019 from the Tokyo University of Agriculture and Technology, Koganei, Japan, where he is currently working toward the postgraduate degree. His research focuses on nonorthogonal multiple access.

Ryota Nakai (Student Member, IEEE) received the B.E. and M.E. degrees in computer and information sciences from the Tokyo University of Agriculture and Technology, Koganei, Japan, in 2017 and 2019, respectively. He is currently working toward the Ph.D. degree with the Institute of Industrial Science, The University of Tokyo, Tokyo, Japan. His research interests include cooperative wireless communications and physical layer security. He was the recipient of the IEEE Vehicular Technology Society Tokyo Chapter 2017 Young Researcher's Encouragement Award, the IEEE Signal Processing Society Japan Student Journal Paper Award in 2019, and the Telecom System Technology Student Award from the Telecommunications Advancement Foundation in 2020.

Shinya Sugiura (Senior Member, IEEE) received the B.S. and M.S. degrees in aeronautics and astronautics from Kyoto University, Kyoto, Japan, in 2002 and 2004, respectively, and the Ph.D. degree in electronics and electrical engineering from the University of Southampton, Southampton, U.K., in 2010.

From 2004 to 2012, he was a Research Scientist with Toyota Central Research and Development Laboratories, Inc., Aichi, Japan. From 2013 to 2018, he was an Associate Professor with the Department of Computer and Information Sciences, Tokyo University of Agriculture and Technology, Tokyo, Japan. Since 2018, he has been an Associate Professor with the Institute of Industrial Science, The University of Tokyo, Tokyo, Japan, where he heads the Wireless Communications Research Group. He has authored or coauthored more than 70 IEEE journal papers. His research interests include wireless communications, networking, signal processing, and antenna technology.

He was the recipient of numerous awards including the Fifth Yasuharu Suematsu Award in 2019, the 33rd Telecom System Technology Award (Honorable Mention) from the Telecommunications Advancement Foundation in 2018, the Sixth RIEC Award from the Foundation for the Promotion of Electrical Communication in 2016, the Young Scientists' Prize by the Minister of Education, Culture, Sports, Science and Technology of Japan in 2016, the 14th Funai Information Technology Award (First Prize) from the Funai Foundation in 2015, the 28th Telecom System Technology Award from the Telecommunications Advancement Foundation in 2013, the Sixth IEEE Communications Society Asia-Pacific Outstanding Young Researcher Award in 2011, the 13th Ericsson Young Scientist Award in 2011, and the 2008 IEEE Antennas and Propagation Society Japan Chapter Young Engineer Award. He was also certified as an Exemplary Reviewer of the IEEE COMMUNICATIONS LETTERS in 2013 and 2014 and the IEEE TRANSACTIONS ON COMMUNICATIONS in 2018. He is currently the Editor of the IEEE WIRELESS COMMUNICATIONS LETTERS.